



PCCP

DNA-RNA hybrid duplexes with decreasing pyrimidine content in the DNA strand provide structural snapshots for the A- to B-form conformational transition of nucleic acids

Journal:	<i>Physical Chemistry Chemical Physics</i>
Manuscript ID:	CP-ART-06-2014-002478.R1
Article Type:	Paper
Date Submitted by the Author:	15-Jul-2014
Complete List of Authors:	Suresh, Gorle; International Institute of Information Technology, CCNSB Priyakumar, U; International Institute of Information Technology, CCNSB

SCHOLARONE™
Manuscripts

Cite this: DOI: 10.1039/c0xx00000x

www.rsc.org/xxxxxx

ARTICLE TYPE

DNA-RNA hybrid duplexes with decreasing pyrimidine content in the DNA strand provide structural snapshots for the A- to B-form conformational transition of nucleic acids

5 Gorle Suresh and U. Deva Priyakumar*

Received (in XXX, XXX) Xth XXXXXXXXX 20XX, Accepted Xth XXXXXXXXX 20XX

DOI: 10.1039/b000000x

DNA-RNA hybrids are heterogeneous nucleic acid duplexes consisting of a DNA strand and a RNA strand, and are formed as key intermediates in many important biological processes. They serve as substrates for the RNase H enzymatic activity, which has been exploited for several biomedical technologies such as antiviral and antisense therapies. To understand the relation of structural properties with the base composition in DNA-RNA hybrids, molecular dynamics (MD) simulations were performed on selected model systems by systematically varying the deoxyypyrimidine (dPy) content from 0 to 100% in the DNA strand. The results suggest that the hybrid duplex properties are highly dependent on their deoxyypyrimidine content of the DNA strand. However, such variations are not seen in their corresponding pure DNA and RNA duplex counterparts. It is also noticed that the systematic variation in deoxyypyrimidine content of hybrids leads to gradual transformation between B- and A-form nucleic acid structures. Binding free energy calculations explain the previous experimental findings that the hybrids with high deoxyypyrimidine content (>50%) are more stable than their respective pure counterparts. Pseudorotation angles, minor groove widths, phosphodiester angles, and glycosidic dihedral angle exhibit gradual A- to A/B-like conformation with decreasing deoxyypyrimidine content. Based on extensive analysis, possible factors that affect RNase H enzymatic activity on hybrid duplexes with high dPy composition are proposed.

20 Introduction

Homogeneous antiparallel DNA duplexes are important in transferring genetic information from DNA to protein by forming Okazaki fragments.¹⁻³ It has been found that heterogeneous nucleic acids namely hybrids and chimeras, containing both DNA and RNA strands within a single duplex exist and are important structural intermediates in certain biological processes.⁴⁻⁹ The DNA-RNA hybrids are duplexes that contain one entire DNA strand complementary to a RNA strand. Chimeras are duplexes that have at least one strand coexisting both DNA and RNA moieties. Processes like DNA replication, transcription, telomerase replication, and reverse transcription⁴⁻⁷ are highly dependent on the formation and cleavage of these novel molecules. Hybrids have been shown to be short lived species that are essential intermediates in several biological processes.¹⁰⁻¹⁵ The presence of two different strands (DNA and RNA) in hybrids results in distinct helical conformation of the hybrids. These hybrids are recognized by RNase H enzyme which is capable of degrading their RNA strand without affecting the complementary DNA strand.^{16,17} The enzymatic (RNase H) recognition is not sequence specific and the enzyme has an extraordinary ability to discriminate DNA-RNA hybrids from other single and double stranded DNA and RNA molecules.

Previous studies have suggested their unique conformation and intermediate minor groove width are possible reasons for this discrimination but the recognition mechanism is still unclear.^{16,17} Since RNA viruses synthesize DNA-RNA hybrids in their reverse transcription process, and since the stability of these molecules is important for their life cycle, it is all more desirable to have a better understanding of the structure-function relationships of hybrid duplexes in general.¹⁸

Discrimination of hybrids from homogeneous duplexes by RNase H enzyme has been exploited for biomedical purposes, such as antisense technology. Numerous studies have been performed on DNA-RNA hybrids not only to understand the structural reasons behind the non-specific recognition but also to explore their potential role in therapeutics.¹⁹ There have been many experimental studies on DNA-RNA hybrids²⁰⁻³⁴ over the past two decades. Initial X-ray crystallographic studies showed that these hybrids exhibit a conformation close to A-form.²⁹⁻³³ But NMR, CD and Raman spectroscopic studies showed that the deoxyriboses in hybrids exist in south conformations and riboses exist in north conformation which attribute A/B-like conformation to hybrids.^{10,11,13,14} Initial computational studies explained the structure of DNA-RNA hybrid supporting the NMR results.³⁵⁻³⁹ These studies suggest that the DNA-RNA hybrids adopt intermediate A/B-like conformation or globally close to A-type conformation.

Previous studies proposed certain factors that may be responsible for the structural discrimination among DNA, RNA and DNA-RNA hybrids, and their biochemical susceptibility in nuclease activity.^{36,40} Minor groove width, helical rise, unique desolvation pattern, conformational sampling of DNA backbone, intrinsic flexibility and deformability have been proposed as possible factors which could play a role in specific discrimination of

*Centre for Computational Natural Sciences and Bioinformatics, International Institute of Information Technology, Hyderabad 500 032, India. Email: deva@iiit.ac.in. Phone: +91-40-6653 1161

† Electronic Supplementary Information (ESI) available: Details about the binding free energy calculations, stiffness analysis, additional figures and tables for hybrids, pure DNA and RNA duplexes. See DOI: 10.1039/b000000x/

antisense oligonucleotides and their biochemical susceptibility.^{36,40} It has been shown experimentally that the hybrid duplexes with high purine composition in their RNA strand show high resistance to nuclease activity.^{12,41} The details of the changes in the structure and dynamics of hybrid duplexes with respect to base composition and how they are recognized by RNase H is not known. The present study aims to address the first aspect by investigating DNA-RNA hybrid duplexes by changing the purine-pyrimidine base composition systematically. Molecular dynamics (MD) simulations are in general useful for studying the dynamics of biological macromolecules like nucleic acids, proteins and their complexes.^{36,42-44} MD simulations in explicit solvent environment have been performed on DNA-RNA hybrids by considering model systems with varying dPy composition in their DNA strand. Several structural and energetic calculations have been done and the results have been compared with their respective B-DNA and A-RNA duplexes. Examination of the current MD results indicates that most of the properties depend on their deoxypyrimidine (dPy) content and reveals possible factors responsible for the nuclease resistance on the hybrid with 100% dPy composition in its DNA strand.

5' -d (CCCTTTTTTCCC) -3'
3' -r (GGGAAAAAAGGG) -5'
100% dPy

5' -d (CGCTTTTTTTCGC) -3'
3' -r (CGCAAAAAAGCG) -5'
75% dPy

5' -d (CGCAAATTTGCG) -3'
3' -r (GCGUUUAAACGC) -5'
50% dPy

5' -d (CGCAAAAAAGCG) -3'
3' -r (GCGUUUUUCGC) -5'
25% dPy

5' -d (GGGAAAAAAGGG) -3'
3' -r (CCCUUUUUUCCC) -5'
0% dPy

Scheme 1: DNA-RNA hybrid duplexes with varying deoxypyrimidine (dPy) composition in their DNA strand. Simulations were also performed on the corresponding five pure DNA and five pure RNA duplexes.

Methods

Model Systems and Sequence Selection: MD simulations were performed on five dodecamer model systems containing 0%, 25%, 50%, 75% and 100% dPy composition in their sequence (Scheme 1). These sequences were selected based on the following criteria: (a) the duplexes must be long enough to form a complete helical turn and (b) contain equal AT/GC (6:6) content. The model sequences considered in this study were taken from available experimental A-RNA structures. MD simulations were also performed on the pure DNA and pure RNA structures with similar sequences except that the thymines (T) in DNA strand were replaced by uracil (U) in RNA strand. This resulted in 15 molecular systems. Additionally, MD simulations were also done on alternating GA sequence to examine the effect of change in sequence on the trends obtained for the model systems used here (Scheme 1).

Simulation protocol: The starting structures corresponding to pure DNA and RNA duplexes were generated using the Sybyl 7.2 software (*Tripos Inc*), and the coordinates for all hybrids were

generated from pure RNA using CHARMM⁴⁵ biomolecular simulation program by performing necessary modifications. A 500 step steepest decent (SD) minimization was performed and the systems were immersed in a pre-equilibrated water box built based on the modified TIP3P model.⁴⁶ The dimensions of the water box were selected so that the distances from non-hydrogen atoms of the nucleic acid duplex are at least 10 Å from the edge of the box and the overlapping water molecules within 2.0 Å of duplex heavy atoms were removed. Sodium ions were placed randomly to neutralize the charge on the systems which were then subjected to 500-step SD and 500-step adopted basis Newton Rapson (ABNR) minimizations with harmonic restraints on heavy atoms, followed by 100 ps MD simulation in NVT ensemble. SHAKE algorithm⁴⁷ was employed to constrain the covalent bonds involving hydrogens. NPT ensemble was used for the production runs using the Nose-Hoover thermostat⁴⁸ for constant temperature and the Langevin piston algorithm⁴⁹ for constant pressure, and periodic boundary conditions were applied throughout the simulations using CRYSTAL module⁵⁰ in CHARMM program. Long range electrostatic interactions were treated using particle mesh Ewald (PME) method.^{51,52} A force switch smoothing function was used from 10 Å to 12 Å for the Lennard-Jones (LJ) interactions,⁵³ while the non-bonded lists were updated heuristically. CHARMM36 all-atom nucleic acid force field⁵⁴⁻⁵⁶ was employed. All the production simulations have been extended upto 100 ns for DNA-RNA hybrid duplexes and 50 ns for regular DNA and RNA duplexes using NAMD⁵⁷ by using the structures obtained at the end of equilibration step. The integration of Newton's equation of motion has been done using the Leapfrog integrator with an integration time step of 2 fs. A weak harmonic restraint of a force constant 4.0 kcal/mol.Å² was applied on the central hydrogen bond of terminal base pairs to prevent the chances of base pair opening⁴² in all the simulations. In addition to CHARMM, visual molecular dynamics (VMD)⁵⁸ and Curves⁵⁹ softwares were also used for performing structural analysis. Details of binding free energy and helical deformation force constant calculations are provided in the Electronic Supplementary Information (ESI).

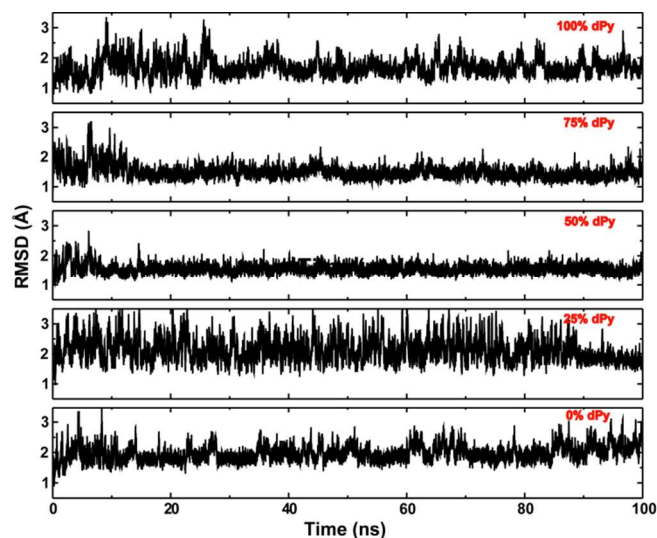


Fig.1 Time evolution of the RMSD (Å) corresponding to five DNA-RNA hybrid duplexes. RMSD plots of the pure DNA and RNA duplexes are presented in Fig. S1 in ESI.

Results and Discussion

Overall structures: To assess the structural changes in simulated systems and to verify the convergence of the simulations, RMSD along the simulation time were computed for all the systems with

respect to their initial conformation. Based on the time series of RMSD of all the hybrids, the structural and energetic analysis were done on the final 80 ns simulation trajectories (37 ns in case of DNA and RNA duplexes) (Fig.1). Visual inspection of the duplexes indicates that the Watson-Crick (WC) base pairing is well preserved throughout the simulations. The RMSD plots corresponding to pure DNA and RNA duplexes indicate that no major changes occur in the overall structure of the duplexes (see Fig. S1 of ESI). The molecular volumes occupied by the duplexes were estimated and are shown in Fig. 2. As the dPy content in hybrid decreases, the occupied volume by the duplexes also decreases. However, such kind of difference in volume change is not observed for pure DNA and RNA duplexes which indicate distinct overall structures of the DNA-RNA hybrid duplexes depend on the base composition which is not seen in case of pure DNA and RNA duplexes.

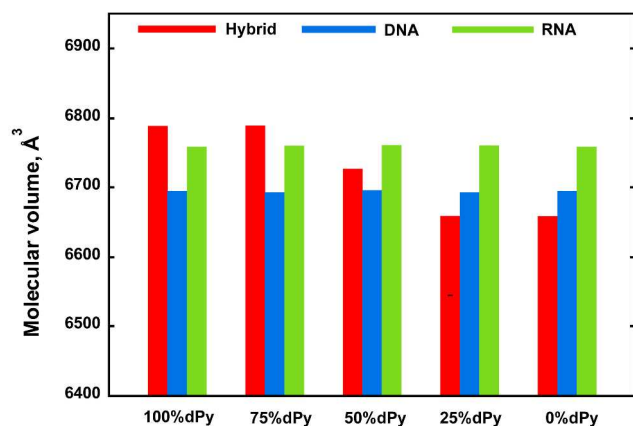


Fig.2 Molecular volume (\AA^3) of DNA-RNA hybrid, DNA and RNA duplexes calculated over the equilibrated trajectory.

Variations in hybrid backbone conformation with the base composition of the DNA strand: Previous EPR and CD experiments on DNA-RNA hybrids have shown that the hybrids (dA-rU) and (dT-rA) exhibit conformations similar to B- and A-type nucleic acid structures respectively.²¹ Moreover, the initial MD simulation results suggested that the duplexes with mixed purine to pyrimidine base composition exhibit conformations intermediate to A- and B-types.³⁶ It has also been shown that while RNA strand in hybrids exhibit conformation similar to pure RNA duplex, the DNA strand exhibit conformational transitions between A- and B-forms.³⁶ The backbone conformation of nucleic acid is mainly dictated by (a) sugar pucker angles (b) α/γ and ε/ζ coupled rotations and (c) glycosidic dihedral angles (χ). It is known that the DNA and RNA duplexes are characterized by deoxyriboses sampling the C2'-endo and riboses sampling the C3'-endo regions respectively. To further understand the preferred conformation of DNA-RNA hybrids, pseudorotation angles corresponding to the furanose sugar pucker were calculated. Probability distributions show that as the number of dPy in hybrid increases, the sampling of the North conformation increases (Fig. 3). It is noticed that this systematic transition in duplex conformation is mostly due to the variation in purine to pyrimidine composition ratio of DNA strand whereas such changes/variations are not observed for RNA strand.

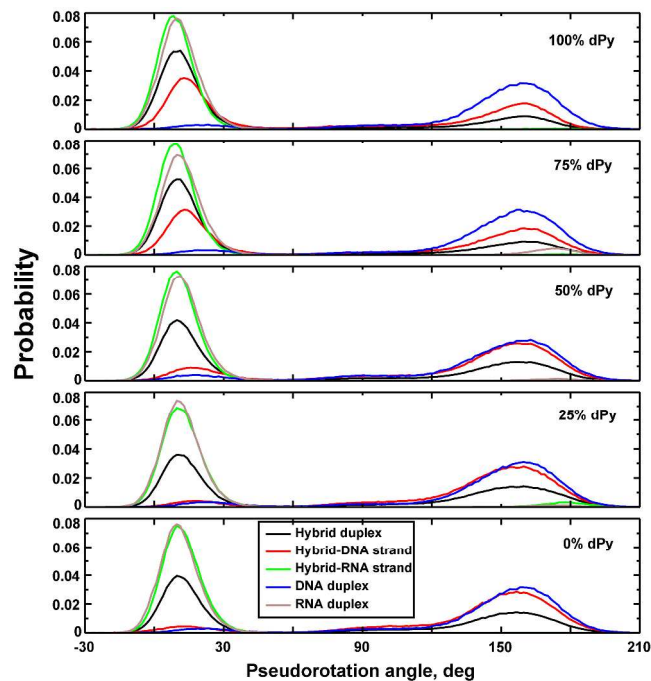


Fig.3 Probability distributions of pseudorotation angles corresponding to the full duplexes and individual strands of DNA-RNA hybrids considered in the present study and their corresponding pure DNA and RNA duplexes.

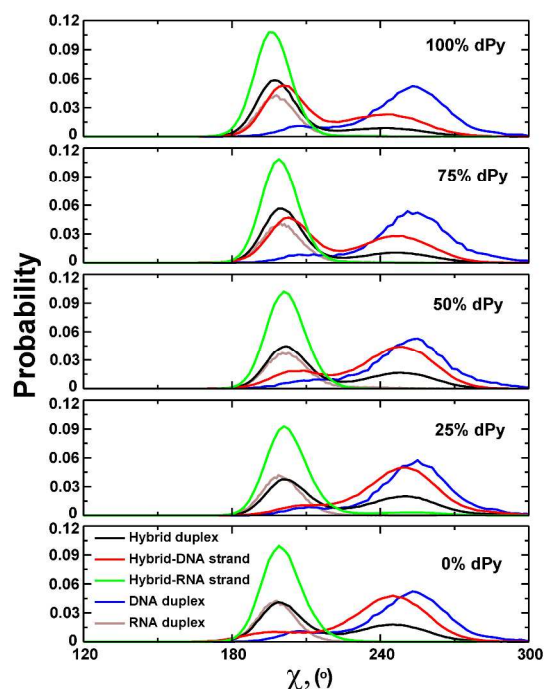


Fig.4 Probability distributions of glycosidic dihedral angle (χ) of sugar-base bond corresponding to the full duplexes and individual strands of DNA-RNA hybrids. Distributions corresponding to pure DNA and pure RNA duplexes are also included for comparison.

Backbone orientations of the nucleic acids play an important role in protein-nucleic acid recognition. Previous studies suggested that sampling of the phosphodiester backbone dihedral angles of hybrids could influence the nuclease activity.³⁶ It is observed from the glycosidic dihedral angle distributions that the low dPy containing hybrids sample conformational regions

similar to high anti similar to pure DNA duplex whereas such sampling is marginal in hybrids with high deoxypyrimidine content (Fig. 4). These probability distributions of glycosidic dihedral angles also indicate a systematic structural transition from A/B-like conformation to A-like conformation with the increase in dPy content in the DNA strand. This further supports that hybrids with high deoxypyrimidine content adopt a backbone conformation similar to that in A-type duplexes. Systematic variations are observed in γ and ξ dihedral angles with the change in dPy composition in DNA strand of DNA-RNA hybrid duplexes (Fig. S4-S5). The probability distributions of ξ dihedral angles indicate that the increase in deoxypyrimidine content increases the sampling region from anti to high anti. The coupled nature of α/γ and ϵ/ξ dihedral angles make the DNA strand flexible to conformational changes with the change in its nucleobase composition.

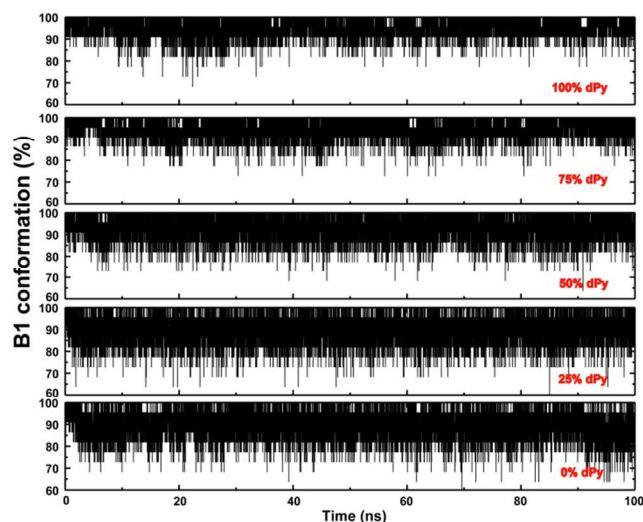


Fig.5 Time series of the percentages of canonical BI conformations in DNA-RNA hybrid duplexes.

BI and BII conformations, exhibited by DNA duplexes can be characterized based on the difference between the ϵ and ξ phosphodiester dihedral angles ($(\epsilon - \xi) > 0$ for BII and $(\epsilon - \xi) < 0$ for BI conformations).^{60,61} Percentages of BI conformation versus BII conformation were calculated for each snapshot (Fig. 5). The data reveal the decrease in BII population with the increase in dPy composition, suggesting more A-like character to the hybrid with 100% dPy composition. The variations observed in sugar pseudorotation angles, glycosidic dihedral angles and backbone dihedral angles together suggest that the DNA-RNA hybrid properties are highly dependent on the base composition and disparities in their properties are well correlated with the base composition present in DNA strand but not in the RNA strand.

Effect of deoxyribose base composition on hybrid internal structure: Asymmetry present in DNA-RNA hybrids attributes unique groove widths compared to respective pure DNA and RNA duplexes.^{35,36} The hybrids have intermediate groove width between DNA and RNA duplex which is proposed to be a factor for the non-specific enzymatic activity of RNase H.¹⁶ The probability distributions of minor groove widths for the hybrids and the corresponding pure duplexes are given in Fig. 6. The

distribution moves towards that of RNA and becomes narrow as the deoxypyrimidine content increases indicating a definite gradual transition from B- to A-form. Possible consequences of such a phenomenon on the lack of nuclease activity on hybrids with high dPy content are discussed later.

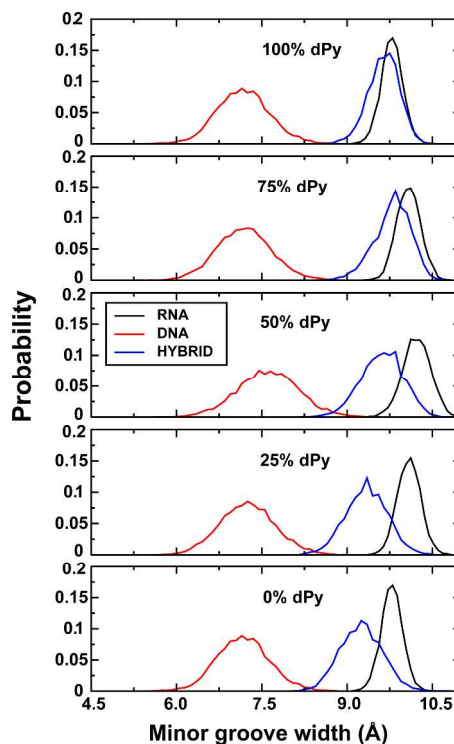


Fig.6 Probability distribution of the minor groove width region of DNA-RNA hybrid, pure DNA and pure RNA duplexes.

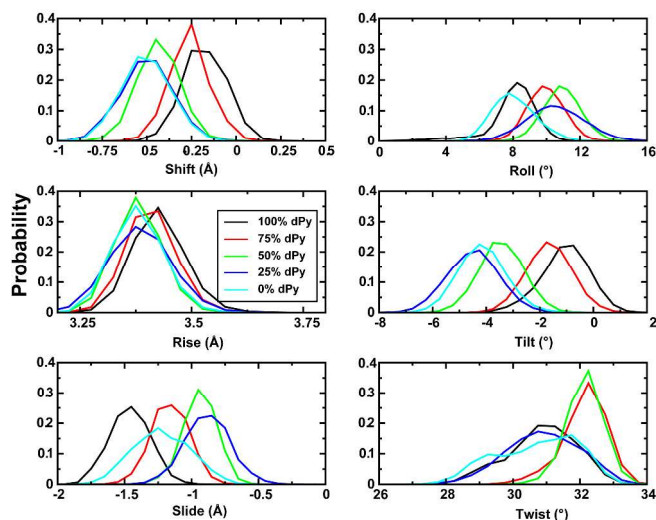


Fig.7 Probability distributions of translational and rotational base pair step parameters of DNA-RNA hybrids.

Local structures of nucleic acid duplexes are best captured by the helical parameters. The calculated translational and rotational parameters corresponding to base pair steps are presented in Fig. 7. The translational parameters shift, rise, the rotational parameter tilt increase with the increase in dPy content. Parameters such as x-displacement, tip, shear, buckle, stagger and propeller-twist

vary systematically with the change in dPy composition (Fig. S6-S7). Such unique helical parameters and deformations could also be possible factors that effect substrate recognition by RNase H.^{36,40} Force constants along the three rotational and translational deformation modes corresponding to base pair steps (Table S1) showed no particular trend in the extent of helical deformations. However, it is observed that hybrids with high dPy content have high global force constant which assign high rigidity to them than other hybrids.

Thermodynamic stability of DNA-RNA hybrids: Free energy calculations corresponding to the formation of duplex from two individual strands can be efficiently used to assess the stability of nucleic acid duplexes in general. MM-GBSA method was used to calculate the free energies of binding, and the differences in the free energies of binding of hybrids with respect to pure nucleic acid counterparts are shown in Fig. 8. The relative binding free energies suggest that all the hybrids are more stable than respective pure DNA counterparts. In contrast, the hybrids exhibit similar thermodynamic stabilities with respect to corresponding RNA when the dPy content is more than 25%. Those with 25% dPy or less were found to be less stable than the RNA counterpart. These results are in excellent agreement with previous experimental studies.¹⁵

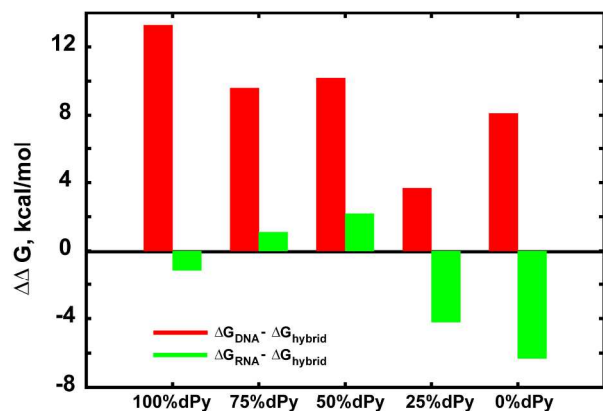


Fig.8 Relative binding free energies of DNA-RNA hybrid duplexes with respect to their corresponding pure DNA and pure RNA duplexes.

Solvent dynamics around the DNA-RNA hybrids: Solvent (water) present around the nucleic acid play a major role in their function and activity, and these interactions play important role in protein-nucleic acid binding. Solvent accessible surface area (SASA) calculations were performed corresponding to various regions of hybrids using a probe radius of 1.4 Å and are shown in Fig.9 and Table S2. The computed SASA values suggest that the hybrids with high dPy composition show distinct solvation patterns compared to other hybrids. As the dPy content increases, the SASA of the DNA strand decreases but that of the RNA strand increases. Such trends are not observed in pure DNA and RNA duplexes (Table S3). To further extend our understanding of the solvation properties of DNA-RNA hybrids, hydration numbers (water molecules whose oxygen atom lies within 3.5 Å of O/N-atoms of the nucleic acid) of duplexes were calculated and are given in Table S4. Consistent with the SASA values, the hydration number values decrease with increase in dPy content especially around their backbone. As the dPy content increases,

the individual DNA and RNA strands show different hydration patterns. Such variations in solvation patterns around the hybrids resultant of the structural changes as discussed in previous subsections are expected to have an impact on the protein-hybrid recognition.

MD simulations have also been performed on 0% and 100% dPy duplexes containing alternating AG sequence (Fig. S2). These simulations have been performed up to 100 ns using similar simulation protocol described in methods section. The calculations such as glycosidic angle, pseudorotation angle and minor groove width regions indicate a similar systematic transition in hybrid conformation (Fig. S3). This suggests that the systematic transition observed in DNA-RNA hybrids with the variation in dPy content of DNA strand is sequence independent and the current conclusions are applicable to all the DNA-RNA hybrid molecules irrespective of the sequence.

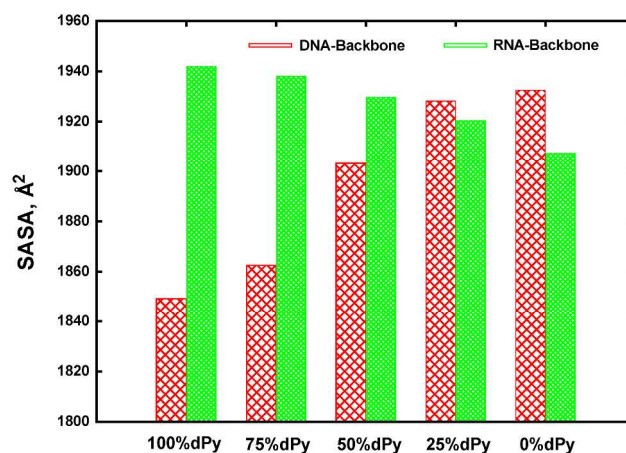


Fig.9 SASA (Å²) values around the backbones of DNA and RNA strands of DNA-RNA hybrid duplexes.

Resistance of hybrid with 100% dPy composition towards nuclease activity: As stated earlier, previous studies showed that hybrids with 100% dPy content are resistant to RNase H hydrolysis similar to pure RNA duplexes.^{12,41} It has also been observed that the RNase H enzyme binds to the hybrid by simultaneously interacting with both the strands carrying the catalytic residues into the right position.¹⁶ Based on the discussions above, we propose two main reasons to why the enzymatic activity is affected with respect to the dPy content. There are two structural properties of such hybrids that exhibit stark similarities with respect to RNA. With respect to increase in the dPy content, the minor groove width increases and exhibits a value similar to RNA when dPy content is 100%. Second is the increased sampling of A-type conformation as against the preference of B-type conformation by DNA strands. Several studies in the past have shown that one of the characteristic of protein-DNA binding is packing of the sugar moieties with certain hydrophobic residues. Such hydrophobic interactions are in general associated with sugar conformations changing from B-type to A-type even in a pure DNA duplex.^{43,62-65} The present analysis such as glycosidic dihedral angles, backbone dihedral angles, and pseudorotation angles suggest almost A-like conformation to the hybrid with 100% dPy composition in its DNA strand. Binding of RNase H is expected to drive the conformation of the hybrid duplex further close to the A-type.

Since the conformation of the hybrid duplex bound to RNase H behaves more like a RNA duplex, the enzyme is not expected to perform the hydrolysis.^{16,17} Other than these two factors, high stability of DNA-RNA hybrids with high dPy composition than their pure counterparts, high desolvation penalty and distinct solvation patterns around the hybrid backbone especially DNA strand could be other possible reasons. Detailed studies on the structure and dynamics of RNase H enzyme bound hybrid duplex are in progress.

10 Conclusions

MD simulations were performed on carefully chosen model systems of the DNA-RNA hybrid duplexes to understand the relationship between base composition and their structural and energetic properties. Comprehensive analyses of the MD trajectories suggest that the properties of DNA-RNA hybrids are highly dependent on their deoxypurine-pyrimidine composition, which is not seen in their corresponding pure counterparts. Furthermore, the structural and energetic properties of hybrid duplexes vary gradually with the systematic change in deoxypyrimidine content in their DNA strand. Free energy calculations showed that hybrid duplexes with increasing number of dPy content are thermodynamically more stable than the respective DNA and RNA duplexes. Distinct features such as sampling of backbone dihedral angles, glycosidic dihedral angles, and furanose sugar puckering suggest that the hybrid with 100% dPy composition exhibits a backbone conformation similar to that of typical A-form nucleic acid, and is proposed as one of the factors for their resistance towards nuclease activity. The transition in minor groove width regions toward typical A-type duplexes also supports this and is likely to be one of the possible factors for their inactivity. This systematic study also reveals the possibility of conceiving stable nucleic acid structures that resemble snapshots during the A- to B-type duplex transformations.

35 Acknowledgements

UDP thanks Prof. Masahiro Ehara, Institute of Molecular Science for his support and encouragement. We thank Department of Biotechnology (DBT), Government of India for financial assistance. GS thanks Council of Scientific and Industrial Research (CSIR), India for senior research fellowship. UDP thanks DBT for the IYBA award.

Notes and references

- 1 B. J. McCarthy and J. J. Holland, *Proc. Natl. Acad. Sci. U. S. A.*, 1965, **54**, 880–886.
- 2 F. H. C. Crick, *Symp. Soc. Exp. Biol.*, 1958, **XII**, 139–163.
- 3 F. Crick, *Nature*, 1970, **227**, 561–563.
- 4 C. K. Mathews, K. E. van Holde and K. G. Ahern, *Biochemistry Benjamin/Cummings*, San Francisco, 2000, Vol. **3**, p876ff.
- 5 M. J. McEachern, A. Krauskopf and E. H. Blackburn, *Annu. Rev. Genet.*, 2000, **34**, 331–358.
- 6 A. J. Rich, *J. Biol. Chem.*, 2006, **281**, 7693–7696.
- 7 A. Rich, *Proc. Natl. Acad. Sci. U. S. A.*, 1960, **46**, 1044–1053.
- 8 E. Zamaratski, P. I. Pradeepkumar and J. J. Chattapadhyaya, *Biochem. Biophys. Methods*, 2001, **48**, 189–208.

- 9 M. Meselson and F. W. Stahl, *Proc. Natl. Acad. Sci. U.S.A.*, 1958, **44**, 671–682.
- 10 J. I. Gyi, G. L. Conn, A. N. Lane and T. Brown, *Biochemistry*, 1996, **35**, 12538–12548.
- 11 A. N. Lane, S. Ebel and T. Brown, *Eur J Biochem.*, 1993, **215**, 297–306.
- 12 S. G. Sarafianos, K. Das, C. Tantillo, Jr. A. D. Clark, J. Ding, J. M. Whitcomb, P. L. Boyer, S. H. Hughes and E. Arnold, *EMBO J.*, 2001, **20**, 1449–1461.
- 13 J. I. Gyi, A.N. Lane, G. L. Conn and T. Brown, *Biochemistry*, 1998, **37**, 73–80.
- 14 J. I. Gyi, D. Gao, G. L. Conn, J. O. Trent, T. Brown and A. N. Lane, *Nucleic Acids Res.*, 2003, **31**, 2683–93.
- 15 E. A. Lesnik, and S. M. Freier, *Biochemistry*, 1995, **34**, 10807–10815.
- 16 M. Nowtony, S. A. Gaidamakov, R. J. Crouch and W. Yang, *Cell*, 2005, **121**, 1005–1016.
- 17 H. Stein and P. Hausen, *Science*, 1969, **166**, 393–395.
- 18 B. Alberts, D. Bray, J. Lewis, M. Raff, K. Roberts, and J. D. Watson, *Molecular Biology of the Cell*, 3rd ed.; Garland Publishing Inc., New York, 1994.
- 19 N. Dias and C. A. Stein, *Mol. Cancer Ther.*, 2002, **1**, 347–355.
- 20 S. Pramanik, S. Nagatoishi, S. Saxena, J. Bhattacharyya, and N. Sugimoto, *J. Phys. Chem. B.*, 2011, **115**, 13862–13872.
- 21 O. Romainczyk, B. Endeward, T. F. Prisner and J. W. Engels, *Mol. Biosyst.*, 2011, **7**, 1050–1052.
- 22 J. T. Olimpo and J. J. DeStefano, *Nucleic Acids Res.*, 2010, **38**, 4426–4435.
- 23 T. Ogawa and T. Okazaki, *Annu. Rev. Biochem.*, 1980, **49**, 421–457.
- 24 Y. Huang, C. Chen and I. M. Russu, *Biochemistry*, 2009, **48**, 3988–3997.
- 25 L. Ratmeyer, R. Vinayak, Y. Y. Zhong, G. Zon and W. D. Wilson, *Biochemistry*, 1994, **33**, 5298–5304.
- 26 B. Rauzan, E. McMichael, R. Cave, L. R. Sevcik, K. Ostrosky, E. Whitman, R. Stegemann, A. L. Sinclair, M. J. Serra and A. A. Deckert, *Biochemistry*, 2013, **52**, 765–772.
- 27 S. Arnott, R. Chandrasekaran, R. P. Millane and H. S. Park, *Biophys J.*, 1986, **49**, 3–5.
- 28 O. Y. Fedoroff, Y. Ge and B. R. Reid, *J. Mol. Biol.*, 1997, **269**, 225–239.
- 29 Y. Xiong and M. Sundaralingam, *Nucleic Acids Res.*, 2000, **28**, 2171–2176.
- 30 S. B. Zimmerman, and B. H. Pfeiffer, *Proc. Natl. Acad. Sci. U. S. A.*, 1981, **78**, 78–82.
- 31 G. L. Conn, T. Brown and G. A. Leonard, *Nucleic Acids Res.*, 1999, **27**, 555–561.
- 32 N. C. Horton and B. C. Finzel, *J. Mol. Biol.*, 1996, **264**, 521–533.
- 33 G. W. Han, M. L. Kopka, D. Langs, M. R. Sawaya and R. E. Dickerson, *Proc. Natl. Acad. Sci. U.S.A.*, 2003, **100**, 9214–9219.
- 34 E. Hantz, V. Larue, P. Ladam, L. Le Moyec, C. Gouyette and T. Huynh Dinh, *Int. J. Biol. Macromol.*, 2001, **28**, 273–284.
- 35 A. Noy, A. Perez, M. Marquez, F. J. Luque and M. Orozco, *J. Am. Chem. Soc.*, 2005, **127**, 4910–4920.
- 36 U. D. Priyakumar and Jr. A. D. MacKerell, *J. Phys. Chem. B.*, 2008, **112**, 1515–1524.
- 37 D. Venkateswarlu, K. E. Lind, V. Mohan, M. Manoharam and D. M. Ferguson, *Nucleic Acids Res.*, 1999, **27**, 2189–2195.
- 38 T. E. Cheatham and P. A. Kollman, *J. Am. Chem. Soc.*, 1997, **119**, 4805–4825.
- 39 S. R. Sanghani and R. Lavery, *Nucleic Acids Res.*, 1994, **22**, 1444–1449.
- 40 A. Noy, J. L. Luque and M. Orozco, *J. Am. Chem. Soc.*, 2008, **130**, 3486–3496.
- 41 H. Huang, R. Chopra, G. L. Verdine and S. C. Harrison, *Science*, 1998, **282**, 1669–1675.
- 42 (a) G. Suresh and U. D. Priyakumar, *J. Phys. Chem. B.*, 2013, **117**, 5556–5564. (b) V. Pande and L. Nilsson, *Nucleic Acids Res.*, 2008, **36**, 1508–1516. (c) G. Suresh and U. Deva Priyakumar, *J. Phys. Chem. B.*, 2014, **118**, 5853–5863.
- 43 U. D. Priyakumar, G. Harika and G. Suresh, *J. Phys. Chem. B.*, 2010, **114**, 16548–16557.

44. (a) U. D. Priyakumar, S. Ramakrishna, K. R. Nagarjuna and S. Karunakar Reddy, *J. Phys. Chem. B.*, 2010, **114**,1707-1718. (b) U. D. Priyakumar, *J. Biomol. Struct. Dyn.*, 2012, **5**, 961-971.
45. B. R. Brooks, C. L. Brooks, III, Jr. A. D. Mackerell, L. Nilsson, R. J. Petrella, B. Roux, Y. Won, G. Archontis, C. Bartels, S. Boresch, A. Cafflich, L. Caves, Q. Cui, A. R. Dinner, M. Feig, S. Fischer, J. Gao, M. Hodosecek, W. Im, K. Kuczera, T. Lazaridis, J. Ma, V. Ovchinnikov, E. Paci, R. W. Pastor, C. B. Post, J. Z. Pu, M. Schaefer, B. Tidor, R. M. Venable, H. L. Woodcock, X. Wu, W. Yang, D. M. York and M. Karplus, *J. Comput. Chem.*, 2009, **30**, 1545–1614.
46. W. L. Jorgensen, J. Chandrasekhar, J. D. Madura, R. W. Impey and M. L. Klein, *J. Chem. Phys.*, 1983, **79**, 926-936.
47. J. P. Ryckaert, G. Ciccotti and H. J. C. Berendsen, *J. Comput. Phys.*, 1997, **23**,327-341.
- 15 48. W.G. Hoover, *Phys. Rev. A.*, 1985, **31**, 1695–1697.
49. S. E. Feller, Y. Zhang, R. W. Pastor and R. W. Brooks, *J. Chem. Phys.*, 1995, **103**, 4613-4621.
50. M. J. Field and M. Karplus, CRYSTAL: Program for Crystal Calculations in CHARMM: Harvard University. Cambridge. MA, 1992.
- 20 51. U. Essmann, L. Perera, M. L. Berkowitz, T. A. Darden, H. Lee and L. G. A. Pedersen, *J. Chem. Phys.*, 1995, **103**, 8577-8593.
52. T. Darden, L. Perera, L. P. Li and L. Pedersen, *Struct. Fold Des.*, 1999, **7**, R55– R60.
- 25 53. P. J. Steinbach and B. R. Brooks, *J. Comput. Chem.*, 1994, **15**, 667-683.
54. N. Foloppe and A. D. MacKerell, *J. Comput. Chem.*, 2000, **21**, 86–104.
55. A. D. MacKerell, and N. K. Banavali, *J. Comput. Chem.*, 2000, **21**,105–120.
- 30 56. E. J. Denning, U. D. Priyakumar, L. Nilsson and A. D. MacKerell, *J. Comp. Chem.*, 2011, **32**,1929-1943.
57. J. C. Phillips, R. Braun, Wei Wang, J. Gumbart, E. Tajkhorshid, E. Villa, C. Chipot, R. D. Skeel, L. Kale and K. Schulten, *J. Comp. Chem.*, 2005, **26**, 1781-1802.
- 35 58. W. Humphrey, A. Dalke and K. Schulten, *J. Molec. Graphics*, 1996, **14**, 33-38.
59. R. Lavery, M. Moakher, J. H. Maddocks, D. Petkeviciute and K. Zakrzewska, *Nucleic Acids Res.*, 2009, **37**, 5917–5929.
- 40 60. B. Hartmann, D. Piazzola and R. Lavery, *Nucleic Acids Res.*, 1993, **21**, 561–568.
61. B. Heddi, N. Foloppe, N. Bouchemal, E. Hantz and B. Hartmann, *J. Am. Chem. Soc.*, 2006, **128**, 9170–9177.
62. L. Dostal, C.Y. Chen, A. H. Wang and H. Welfle, *Biochemistry*, 45 2004, **43**, 9600-9609.
63. L. Chen, Q. C. Zheng, L. Y. Yu, W. T. Chu, J. L. Zhang, Q. Xue, H. X. Zhang and C. C. Sun, *J. Biomol. Struct. Dyn.*, 2012, **30**, 716-727.
64. L. Chen, J. L. Zhang, L.Y. Yu, Q. C. Zheng, W.T. Chu, Q. Xue, H. X. Zhang and C. C. Sun, *J. Phys. Chem. B.*, 2012, **116**,12415-12425.
- 50 65. C.Y. Chen, T. P. Ko, T. W. Lin, C. C. Chou, C. J. Chen and A. H. Wang, *Nucleic Acids Res.*, 2005, **14**, 430-438.

55